Design and Optimization of a Compact Bio-Inspired Microstrip Antenna at 2.4 GHz for WBAN Applications with Machine Learning based S11 Prediction

¹Nagaveni C R, ²Anandaraju M B, ³Swetha Amit and ⁴Rajendra Soloni

^{1, 2}Department of Electronics and Communication Engineering, BGS Institute of Technology, Adichunchanagiri University, BG Nagara, Mandya, India.

³SmartBeam Resonetics, Bengaluru, Karnataka, India.

⁴Department of Electronics and Communication Engineering, Jain Institute of Technology, Davangere, Karnataka, India.
¹nagaveniecdept@gmail.com, ²mb.anandaraju@gmail.com, ³swetha.amit@gmail.com, ⁴rajendrasoloni@gmail.com

Correspondence should be addressed to Nagaveni C R: nagaveniecdept@gmail.com

Article Info

ISSN: 2788-7669

Journal of Machine and Computing (https://anapub.co.ke/journals/jmc/jmc.html)

Doi: https://doi.org/10.53759/7669/jmc202606004

Received 02 May 2025; Revised from 15 August 2025; Accepted 01 October 2025.

Available online 14 October 2025.

©2026 The Authors. Published by AnaPub Publications.

This is an open access article under the CC BY-NC-ND license. (https://creativecommons.org/licenses/by-nc-nd/4.0/)

Abstract – This study introduces a novel bio-inspired microstrip patch antenna operating at 2.4 GHz, optimized for Wireless Body Area Network (WBAN) applications through integration with machine learning-based analysis. The antenna features a papaya leaf-inspired radiating element and incorporates two circular slots within a defected ground plane to enhance impedance matching and achieve substantial miniaturization. Fabricated on an FR-4 substrate (dielectric constant: 4.4, loss tangent: 0.02), the device achieves a compact footprint of 53.32 × 32.13 × 1.58 mm³. The leaf-shaped design maximizes effective perimeter while minimizing the physical size, leading to improved radiation efficiency and performance in constrained environments. To accelerate performance evaluation and design iteration, a Random Forest Regression algorithm is implemented for predictive modeling of the S11 reflection coefficient. The model achieves a high degree of accuracy (R² = 0.9015) in mapping the complex behavior of reflection loss, demonstrating its efficacy for ISM band services such as Wi-Fi, WiMAX, and Bluetooth communications. Comparative analysis between simulation and experimental results is conducted, including investigations of substrate variation (PDMS) and impact of slot geometry on antenna performance. The prototype is further integrated with a transceiver module and validated for real-time WBAN scenarios. By embedding a data-driven approach into the design workflow, reliance on computationally expensive electromagnetic simulations is reduced, enabling rapid optimization and deployment of advanced antenna systems for biomedical and wearables applications.

Keywords – Bio-Inspired Microstrip-Patch Antenna, Defected Ground Structure (DGS), Wireless Body Area Network (WBAN), High Frequency Structure Simulator (HFSS), Specific Absorption Rate (SAR), Random Forest Regressor.

I. INTRODUCTION

Conventional antennas often struggle to achieve optimal gain, bandwidth, compactness, and radiation patterns. Bio-inspired antennas, drawing design inspiration from natural structures like leaves, feathers, and fractals, offer a compact alternative with up to 50% size reduction while enhancing performance. In response to the escalating requirements for high-performance wireless communication, these antennas are particularly well-suited for utilization in Wireless Body Area Networks (WBANs), facilitating efficient and reliable data transmission for diverse body-centric applications. Operating within the IEEE 802 standards, particularly the widely used 2.4 GHz ISM band, WBANs enable real-time health monitoring through wearable and implantable medical devices. This technology supports applications in telemedicine, patient tracking, rehabilitation monitoring, and remote healthcare, improving accessibility and efficiency. Research on compact and efficient antennas for 2.4 GHz ISM band applications has led to various innovative designs. Past researchers [1] developed a circular patch antenna for Wi-Fi and WLAN, enhancing efficiency and bandwidth. Focused on a wearable WBAN antenna [2], emphasizing flexibility and stable performance on the human body. Past researchers [3] introduced a bio-inspired wideband antenna using perturbation techniques for improved radiation characteristics. And [4] designed a high-gain, circularly

polarized slot antenna, demonstrating enhanced bandwidth and polarization. These studies provide a Conventional antenna often struggle to achieve optimal gain, bandwidth, compactness, and radiation patterns. Bio-inspired antennas, drawing design inspiration from natural structures like leaves, feathers, and fractals, offer a compact alternative with up to 50% size reduction while enhancing performance. In response to the escalating requirements for high-performance wireless communication, these antennas are particularly well-suited for utilization in Wireless Body Area Networks (WBANs), facilitating efficient and reliable data transmission for diverse body-centric applications. Operating within the IEEE 802 standards, particularly the widely used 2.4 GHz ISM band, WBANs enable real-time health monitoring through wearable and implantable medical devices. This technology supports applications in telemedicine, patient tracking, rehabilitation monitoring, and remote healthcare, improving accessibility and efficiency. Research on compact and efficient antennas for 2.4 GHz ISM band applications has led to various innovative designs. Past researchers [5][6] designed a high-gain, circularly polarized slot antenna, demonstrating enhanced bandwidth and polarization. These studies provide a foundation for advancing bio-inspired antennas, defected ground structures (DGS), and machine learning-based optimizations for WBAN and IoT applications. The bio-inspired antenna, operating at 2.4 GHz, is integrated with an ESP32-based WBAN system for real-time health monitoring using biomedical sensors. A DGS with circular slots enhances impedance matching and radiation efficiency while maintaining compactness. Machine learning-based optimization, using Random Forest Regression, improves the S11 parameter, reducing reliance on extensive electromagnetic simulations and ensuring optimal performance for medical and sports applications. Substrate materials significantly impact microstrip antenna performance, affecting impedance matching, radiation efficiency, and flexibility. FR-4, a cost-effective substrate with dielectric constant 4.4 and loss tangent of 0.02 is used. The bio-inspired antenna's performance is evaluated by analyzing return loss, gain, and suitability for WBAN applications. The antenna utilizes a DGS with slots in the ground plane to enhance impedance matching, reduce mutual coupling, and suppress unwanted signals. This improves radiation efficiency and minimizes outof-band interference. Electromagnetic simulations carried out in HFSS 2024R provide detailed analysis of crucial antenna parameters, including S-parameters and field distributions, while Specific Absorption Rate (SAR) assessment involving a human phantom model enables verification against safety guidelines for wearable, on-body applications.

The remainder of the paper is organized as follows: Section 2 and 3 presents the proposed methodology. Section 4 provides an overview of the results. Section 5 provides an analysis of the results with machine learning. Section 6 contains the work's conclusion.

II. DESIGN AND STRUCTURAL CONFIGURATION OF THE ANTENNA

The proposed microstrip antenna, inspired by the Carica Papaya leaf, is designed for 2.4 GHz applications, including WBANs, ISM band communications, Wi-Fi, Wi-Max, and Bluetooth. The bio-inspired shape enhances performance by increasing the effective perimeter while maintaining compact dimensions, improving radiation characteristics and impedance matching. Featuring overall dimensions of $53.32 \times 32.13 \times 1.58$ mm³, the antenna demonstrates a reduced physical footprint while sustaining high radiation efficiency, making it well-suited for space-constrained wearable applications. The design starts with a circular microstrip patch due to its ease of analysis, simple fabrication, and favourable radiation properties. The initial radius (R) of 11.7 mm is determined using equations ((1) to (10) that consider operating frequency (f), dielectric constant (ϵ_r), and substrate height (h). This circular patch is then modified into a papaya leaf-inspired shape to enhance bandwidth and impedance matching, making it more efficient for RF applications.

Radius (R)=
$$f/\sqrt{(1+2h)/(\pi\epsilon \ r F\{ln \ [(E\pi/2h)+1.7726]))}$$
 (1)

$$F = (8.791 \times [10] ^9) / (f_r \sqrt{(\epsilon_r)})$$
 (2)

Where h is the height of the substrate ϵ_r is the dielectric constant and fr is the resonant frequency. A papaya leaf has a lobed, segmented structure with central symmetry. This can be modeled using a modified polar equation that introduces leaf-like lobes and veins as in equation 3.

$$r(\theta) = R \left(1 + \alpha \sin \left(m\theta \right) + \beta \left[\cos \right] ^n \left[(\theta/2) \right)$$
(3)

 $r(\theta)$ defines the radial distance at angle θ , outlining the leaf shape, R is the base radius of the circular antenna, α controls the depth of the lobes, m defines the number of lobes and β adjusts the smooth curvature along the leaf veins and n controls how sharply the edges taper. The resonance frequency can be calculated from the equation 4.

$$f_r=C/(2L_eff [v_{\epsilon}] _eff)$$
 (4)

(4) fr is the resonance frequency, c is the speed of light in a vacuum and Leff is the effective path length along the structure, estimated by as shown in equation 5.

$$L \text{ eff}=\pi R(1+\alpha/2+\beta/4) \tag{5}$$

seff is effective dielectric constant is calculated by equation 6 and 7 where Weff if the effective width

$$\varepsilon \text{ eff}=(\varepsilon \text{ r+1})/2+(\varepsilon \text{ r-1})/2 (1+12\text{h/W eff})^{-(-1/2)}$$
 (6)

$$W eff = 2R (1 + \alpha)$$
 (7)

Gain represents the antenna's ability to direct input power in a particular direction, combining both directivity and efficiency as in equation 8

$$G(\theta, \phi) = D(\theta, \phi) \times \eta$$
 (8)

 $G(\theta, \phi)$ is the gain at angles θ and ϕ , $D(\theta, \phi)$ is the directivity, which HFSS calculates and η is the radiation efficiency, defined as in equation 9

$$\eta = P \operatorname{rad}/P \operatorname{input}$$
 (9)

HFSS provides the total gain in dB as in equation 10

$$G_dB=10 \quad \llbracket \log \rrbracket \quad 10 \quad \llbracket (G(\theta,\emptyset) \rrbracket \tag{10}$$

The defected ground structure (DGS) is realized by etching symmetrical slots on both sides of the ground plane, with each slot measuring 23.4 mm by 18 mm, thereby optimizing the antenna's electromagnetic response. Additionally, a rectangular strip is integrated within the defected ground plane to enhance bandwidth and improve impedance matching. The introduction of a ring resonator within the ground plane significantly alters the antenna's electrical properties, as ring resonators exhibit frequency-selective behaviour by modifying the effective capacitance and inductance of the transmission line. This alteration influences the surface current distribution, optimizing the S-parameters and achieving resonance precisely at 2.4 GHz. The inclusion of circular slots within the ground structure significantly contributes to the improvement of the antenna's gain and radiation efficiency by optimizing current distribution and enhancing electromagnetic performance. These concentric circular slots, with radii of 0.8 mm and 1 mm, introduce additional electromagnetic coupling, thereby refining the excitation and propagation of electromagnetic waves within the substrate. The defected ground plane disturbs the conventional current flow, leading to controlled excitation and guided wave propagation, which in turn enhances the overall antenna performance by increasing gain, suppressing higher-order harmonics, and reducing cross-polarization effects. The circular patch, having an initial radius of 11.7 mm, is further modified into a papaya leafinspired shape to enhance bandwidth and impedance matching, making it more efficient for RF applications. At the same design frequency, the circular patch antenna is 16% smaller than the rectangular patch antenna [7][8]. The circular patch serves as the foundational element for designing bio-inspired antennas modeled after papaya leaves, which are precisely shaped using polylines within the HFSS simulation environment. Fig 1 represents the top and bottom view of the suggested antenna while the **Table 1** outlines the design parameters and dimensions.

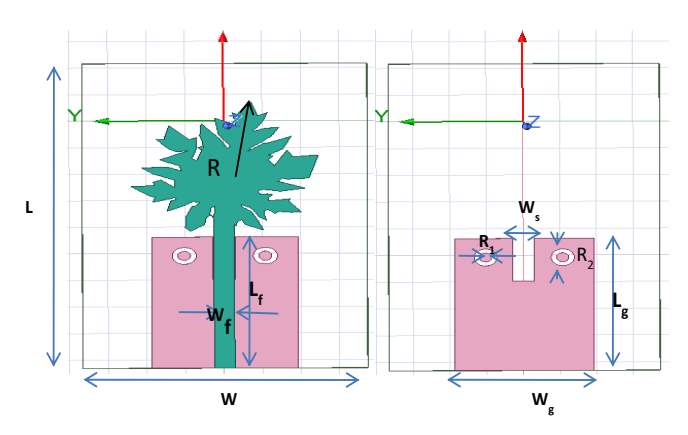


Fig 1. (a) Top View (b) Bottom View of The Proposed Antenna.

Table 1. Proposed Bio-Inspired Papaya Shaped Antenna Design Parameters (In Mm)

Description	Value (in mm)
Radius of the circular patch initiator (R)	11.7
Length of substrate (L)	53.32

Width of substrate (W)	32.13
Height of substrate (h)	1.58
Width of feedline (W _f)	2.52
Length of feedline (L _f)	27
Width of ground plane (Wg)	18
Length of ground plane (Lg)	23.4
Width of rectangular strip (W _s)	2.7
Radius of concentric circle 1 (R ₁)	0.8
Radius of concentric circle 2 (R ₂)	1

III. RF TRANSCEIVER

A papaya leaf-shaped antenna integrated with an ESP32 and biomedical sensors enables real-time health monitoring. The ESP32 processes physiological data and transmits it wirelessly via Wi-Fi and Bluetooth for efficient health tracking. The bio-inspired papaya leaf-shaped antenna enhances wireless communication by optimizing gain, signal strength, and interference reduction. It supports multi-band operation, ensuring efficient data transmission and less energy usage for continuous health monitoring. At the receiver end, a transceiver captures and decodes the transmitted health data for real-time display. The system enables continuous monitoring and can trigger alerts for abnormal readings, enhancing critical health tracking. The integrated system enables efficient, low-latency wireless health monitoring. Its compact, energy-efficient design makes it ideal for wearable healthcare applications. The integration of the recommended antenna for signal transmission and reception is shown in Fig 2.

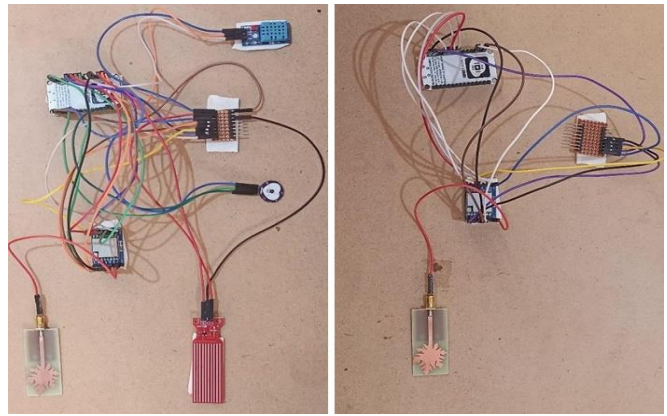


Fig 2. Integration of the Bio-Inspired Antenna into the Hardware System (a) Transmitter (b) Receiver.

IV. RESULT AND DISCUSSIONS

The antenna simulation and analysis using HFSS confirm resonance at 2.4 GHz. Concentric circular DGS (0.8mm and 1mm) enhances radiation efficiency and improves return loss characteristic (S11 = -22.81 dB) as represented in **Fig 3**. The VSWR of 1.25 (presented in **Fig 4**) at 2.4 GHz ensures effective impedance matching.

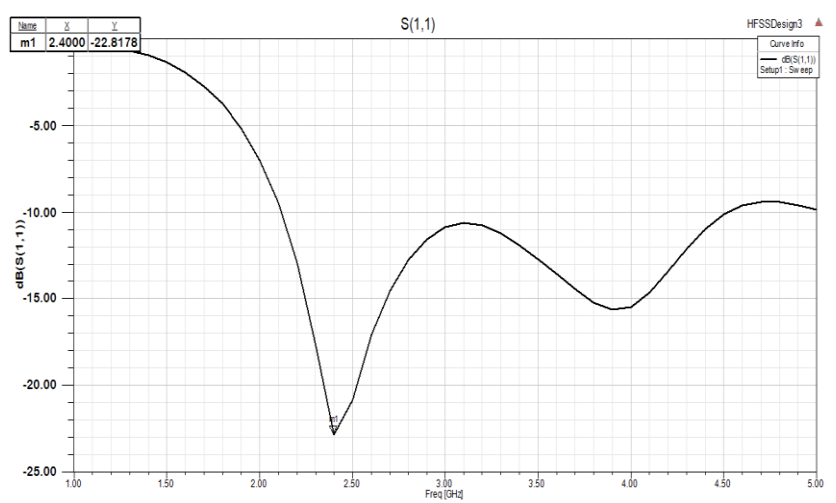


Fig 3. Return Loss in dB (S₁₁).

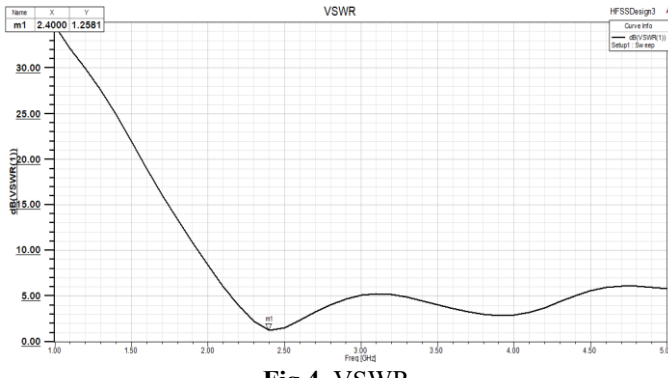


Fig 4. VSWR.

The radiation pattern and the gain of the projected antenna at 2.4 GHz is illustrated in the **Fig 5 and 6** respectively. The radiation pattern at both the E-plane ($\Phi = 00$) and H-plane ($\Phi = 900$) are quasi–Omni directional and can be suitable for WBAN applications. The projected antenna has a gain of 3.4 dB.

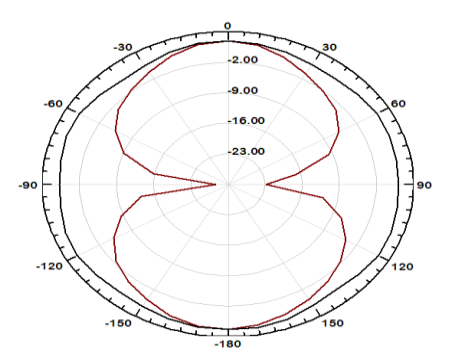


Fig 5. Radiation Pattern.

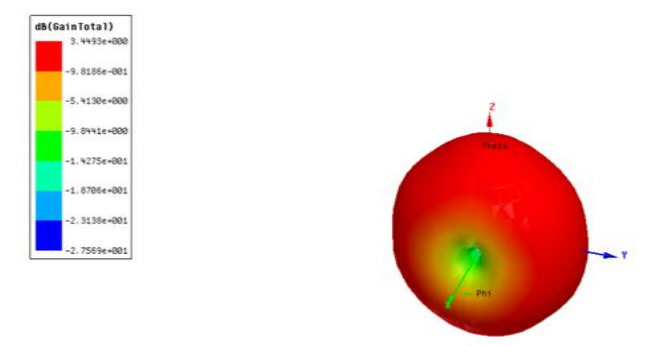


Fig 6. Gain in dB.

The recommended antenna is fabricated on the FR4 substrate is presented in **Fig 7**. The simulation and fabricated results have been tabulated in **Table 2**. The compact size of the antenna makes it possible to use as wearable antenna. Since the outcomes match the simulated design, they can be applied in real-world scenarios.



Fig 7. Fabricated Antenna.

The bio-inspired papaya leaf-shaped antenna was experimentally validated using a Vector Network Analyzer (VNA) to measure return loss across 1–6 GHz (shown in **Fig 8**). The fabricated design closely matched simulations, confirming improved resonance, radiation efficiency, and impedance- matching with DGS integration.

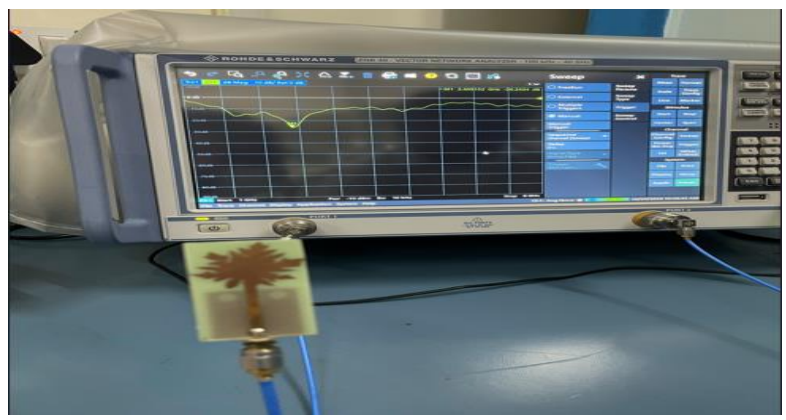


Fig 8. Measurement of S11 using a VNA.

The Fig 9 presents the S11 plot of the fabricated antenna, demonstrating a resonance at 2.405 GHz with a deep notch of -26.24 dB.

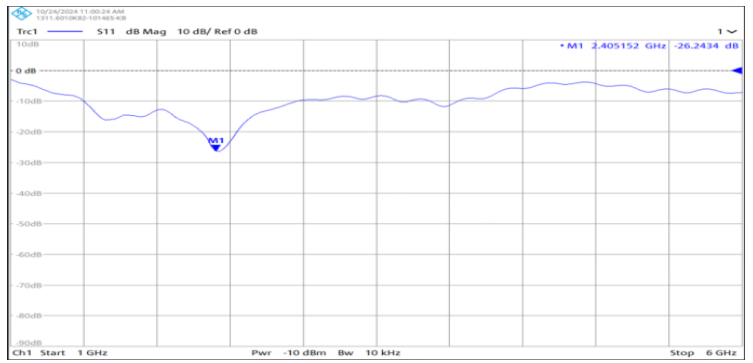


Fig 8. S11 for Fabricated Antenna.

The comparison between the simulated and fabricated antenna parameters as shown in Table 2.

Table 3. Comparative Analysis

Sl. No	Antenna Parameters	Simulated	Fabricated
1	Operating Frequency	2.4 GHz	2.405 GHz
2	VSWR	1.25	1.10
3	Return loss	-22.81dB	-26.24dB

Table 3 provides a comparative analysis of various configurations of the bio-inspired papaya leaf-shaped antenna, focusing on the influence of different substrate materials on its performance characteristics and design modifications on key performance parameters such as S11 and gain.

Table 3. Comparative Analysis

Substrate	Substrate dimension	S ₁₁ (dB)	Gain(B
FR4 Epoxy	25 x 20 x 1.5mm ³	-52.89	1.98
PDMS	33 x 30 x 1 mm ³	-26.82	1.9
FR4 Epoxy	$59.25 \times 35.7 \times 1.58 \text{ mm}^3$	-20	3.13
FR4 Epoxy	76 x 88 x 0.3 mm ³	-1.1505	2.77
FR4 Epoxy (Proposed)	53.32 × 32.13 × 1.58 mm ³	-22.81	3.4

SAR measures RF energy absorption in human tissues, crucial for ensuring safe WBAN antenna performance. Simulations in HFSS assess SAR impact, helping optimize antenna placement to minimize exposure while maintaining communication efficiency [9][10]. **Table 4** presents the SAR values and corresponding gain for different gaps between the antenna and the human phantom. In order to reduce SAR to standard rate and to increase gain metamaterials structures can be used in between antenna and phantom as future work.

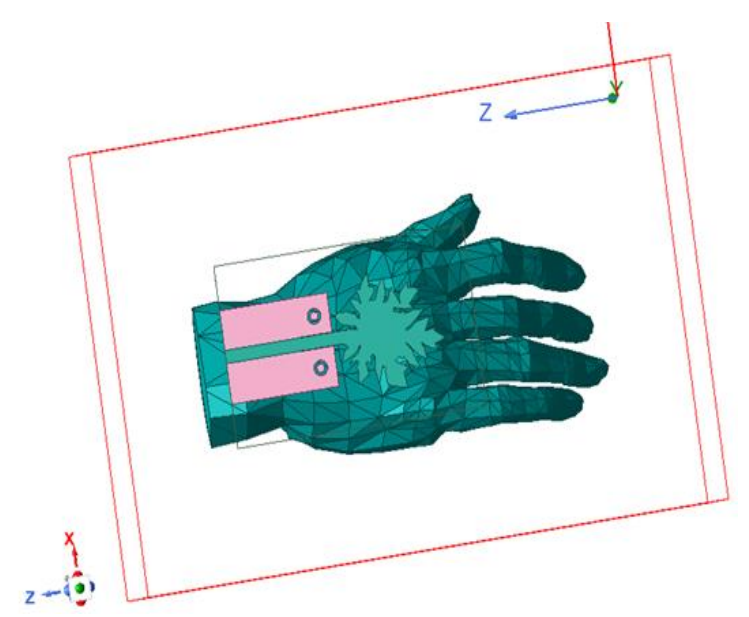


Fig 9. Bio-Inspired Antenna on Phantom.

Tab	le 4.	Gain	and S	SAR	For	Different	Gaps	Between	Phantom	and a	Antenna
-----	-------	------	-------	-----	-----	-----------	------	---------	---------	-------	---------

SI. No	Gap in mm	SAR in (W/kg)	Gain
1	0.5	38.64	-4.13
2	1	37.764	-4.24
3	2	31.933	-3.8
4	2.24	30.85	-4.04
5	3.01	27.369	-3.85
6	3.5	25.462	-3.66
7	4	22.907	-3.52
8	5	19.884	-3.34
9	6	17.821	-3.26

V. ANALYSIS OF S11 PARAMETER PREDICTION USING MACHINE LEARNING

Random Forest (RF) is an ensemble learning algorithm that builds multiple decision trees during the training phase. For regression tasks, the model predicts outcomes by averaging results from all individual trees, whereas for classification tasks, it employs majority voting to determine the final class. A key hyperparameter, ntrees, defines the total number of trees within the forest. Each tree is trained on distinct subsets of data, introducing diversity that enhances the model's ability to generalize [11][12][13]. As an ensemble of decision trees, RF effectively combines numerous weak learners to form a strong, robust predictive model widely used in antenna design optimization for accurately forecasting performance metrics and accelerating the design process. In antenna design, RF has been effectively applied to predict vital performance metrics such as the S11 parameter (return loss), which is essential to evaluate impedance matching and antenna efficiency. By learning from either simulated or experimental datasets, the RF model can accurately estimate S11 values depending on design variables, significantly aiding the antenna optimization process. This predictive capability proves especially useful in parametric studies of advanced antenna geometries, including bio-inspired or metamaterial configurations, where multiple design factors influence overall performance. This machine learning methodology not only expedites the prediction of antenna performance but also diminishes dependence on computationally intensive electromagnetic simulations, thereby enabling more rapid and efficient iterative design processes. The Random Forest model captures these nonlinear relationships without assuming any explicit functional form, making it a powerful tool in the iterative optimization of antenna structures. The study uses a Random Forest Regressor [14] to predict the S11 parameter of a bioinspired antenna at 2.4 GHz. The model, trained using measured S11 data, demonstrates high accuracy, as confirmed by evaluation metrics such as Mean Absolute Error (MAE), Mean Squared Error (MSE), Root Mean Squared Error (RMSE), and the Coefficient of Determination (R2). A scatter plot comparison (as shown in Fig 11) confirms the model's accuracy

in predicting S11 values, reducing reliance on simulations. This data-driven approach streamlines bio-inspired antenna design, enabling efficient optimization and rapid prototyping for wireless applications.

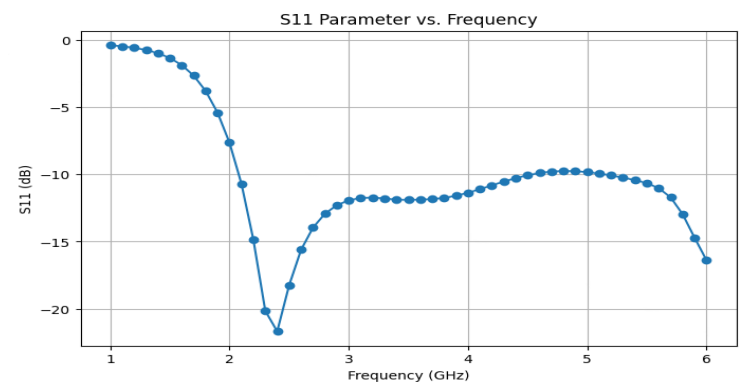


Fig 10. S11 Parameter vs. Frequency Response.

The S11 vs. frequency plot shows a strong resonance at 2.4 GHz with an S11 of -22 dB (as shown in Fig 10), ensuring good impedance matching. This confirms the antenna's efficiency for Wi-Fi, Bluetooth, and ISM band applications. The RF model provides precise predictions of the S11 parameter, showing a high correlation between the measured and estimated values as shown in Fig 11. In antenna design, this approach has been effectively utilized to forecast critical performance indicators like S11 (return loss), which is essential for analyzing impedance matching and antenna efficiency. Low MAE (0.7166 dB) and RMSE (1.3827 dB) confirm minimal prediction errors, ensuring reliable reflection coefficient estimation [15]. The Random Forest model achieves an R² score of 0.9015, accurately predicting the S11 parameter with minimal variance. This data-driven approach accelerates antenna design by reducing reliance on time-consuming electromagnetic simulations.

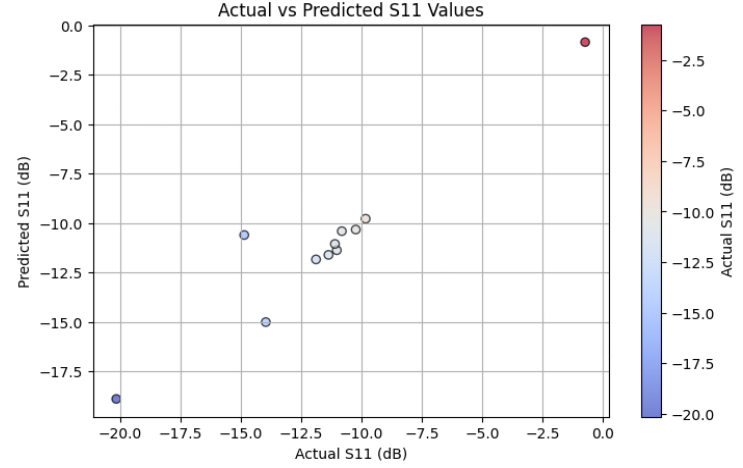


Fig 11. Comparison of Actual Vs. Predicted S11 Values.

VI. CONCLUSION

A bio-inspired papaya leaf-shaped antenna (53.32×32.13×1.58 mm³) was designed, simulated, and fabricated for WBAN applications. FEM analysis in HFSS with DGS integration achieved a 2.4 GHz resonance, S11 of -22.81 dB, and VSWR of 1.2 5. Experimental validation via VNA confirmed performance with a slight frequency shift to 2.405 GHz, improved S11 of -26.24 dB, and a quasi-omnidirectional radiation pattern. Simulated and actual S11 values aligned, confirming the model's reliability for wearable applications. Future work will focus on multi-band optimization and SAR reduction using metamaterials.

CRediT Author Statement

The authors confirm contribution to the paper as follows:

Conceptualization: Nagaveni C R, Anandaraju M B, Swetha Amit and Rajendra Soloni; Methodology: Nagaveni C R and Anandaraju M B; Software: Swetha Amit and Rajendra Soloni; Data Curation: Nagaveni C R and Anandaraju M B; Writing- Original Draft Preparation: Nagaveni C R, Anandaraju M B, Swetha Amit and Rajendra Soloni; Visualization: Nagaveni C R and Anandaraju M B; Investigation: Swetha Amit and Rajendra Soloni; Supervision: Nagaveni C R and Anandaraju M B; Validation: Swetha Amit and Rajendra Soloni; Writing- Reviewing and Editing: Nagaveni C R,

Anandaraju M B, Swetha Amit and Rajendra Soloni; All authors reviewed the results and approved the final version of the manuscript.

Acknowledgements

The authors would like to express their sincere gratitude to the institute and its faculty for their invaluable support and encouragement in conducting this research. They also extend their appreciation to the facility in Bengaluru for assisting with the fabrication process and to MSRIT, Bangalore, for providing the resources and environment for antenna testing.

Data Availability

The data set used in the paper is in the link provided https://drive.google.com/file/d/1Kb_oaZ8My4RXZd7leumREy-MswQJR7ZS/view?usp=drive link

Conflicts of Interests

The author(s) declare(s) that they have no conflicts of interest.

Funding

No funding agency is associated with this research.

Competing Interests

The authors declare no conflict of interest, financial or otherwise.

References

- [1]. K. P. Lad, K. Mhapsekar, and S. Baudha, "A Compact Circular Patch Antenna for 2.4 GHz Wi-Fi and Other WLAN Applications," 2022 IEEE Microwaves, Antennas, and Propagation Conference (MAPCON), pp. 716–718, Dec. 2022, doi: 10.1109/mapcon56011.2022.10046876.
- [2]. T. Zerith M and N. M, "A Compact Wearable 2.45 GHz Antenna for WBAN Applications," 2020 5th International Conference on Devices, Circuits and Systems (ICDCS), pp. 184–187, Mar. 2020, doi: 10.1109/icdcs48716.2020.243577.
- [3]. J. O. Abolade, D. B. O. Konditi, and V. M. Dharmadhikary, "Bio-inspired wideband antenna for wireless applications based on perturbation technique," Heliyon, vol. 6, no. 7, p. e04282, Jul. 2020, doi: 10.1016/j.heliyon.2020.e04282.
- [4]. V. A. S. Ponnapalli, Sowjanya, R. Sudutha, N. Abhishek, and K. S. Pranitha, "Design of Bio Inspired Maple Leaf Microstrip Patch Antenna Array with Different Substrates for Wireless Applications," 2021 International Conference on Recent Trends on Electronics, Information, Communication & Communica
- [5]. Z. Iqbal and S. Lim, "Design of a High-Gain, Wideband, Circularly Polarized Slot Antenna," 2019 IEEE International Symposium on Antennas and Propagation and USNC-URSI Radio Science Meeting, pp. 1921–1922, Jul. 2019, doi: 10.1109/apusncursinrsm.2019.8888874.
- [6]. Indrasen Singh and Dr. V.S. Tripathi, "Micro strip Patch Antenna and its Applications: a Survey", Int. J. Comp. Tech. Appl., Vol 2 (5), pp.1595-1599
 [7]. B. Hu, G.-P. Gao, L.-L. He, X.-D. Cong, and J.-N. Zhao, "Bending and On-Arm Effects on a Wearable Antenna for 2.45 GHz Body Area
- [7]. B. Hu, G.-P. Gao, L.-L. He, X.-D. Cong, and J.-N. Zhao, "Bending and On-Arm Effects on a Wearable Antenna for 2.45 GHz Body Area Network," IEEE Antennas and Wireless Propagation Letters, vol. 15, pp. 378–381, 2016, doi: 10.1109/lawp.2015.2446512.
- [8]. B. Barik, A. Kalirasu, and A. V. P. Kumar, "Design and Performance Analysis of 2.4 GHz Microstrip Patch Antenna," 2021 2nd International Conference for Emerging Technology (INCET), pp. 1–6, May 2021, doi: 10.1109/incet51464.2021.9456148.
- [9]. P. Mahajan, A. Vashistha, and S. Pani, "Performance Analysis of Circular Patch Array Antenna for WLAN Application," 2021 8th International Conference on Signal Processing and Integrated Networks (SPIN), pp. 1114–1118, Aug. 2021, doi: 10.1109/spin52536.2021.9565971.
- [10]. H. Nornikman et al., "Dual Circular-Polarized Slot Antenna Design for Wireless MIMO System at 2.4 GHz," 2018 International Conference on Electrical Engineering and Computer Science (ICECOS), pp. 19–24, Oct. 2018, doi: 10.1109/icecos.2018.8605228.
- [11]. P. Reis and H. G. Virani, "Design of a Compact Microstrip Patch Antenna of FR-4 Substrate for Wireless Applications," 2020 International Conference on Electronics and Sustainable Communication Systems (ICESC), pp. 713–716, Jul. 2020, doi: 10.1109/icesc48915.2020.9156024.
- [12]. J.C Wang, E.G. Lim. Leach, Z. Wang and K.L Man, "Review of wearable antennas for WBAN applications IAENG International Journal of Computer Science, 43:4,IJCS_43_4_10
- [13]. M. N. Suma, R. K. Raj, M. Joseph, P. C. Bybi, and P. Mohanan, "A compact dual band planar branched monopole antenna for DCS/2.4-GHz WLAN applications," IEEE Microwave and Wireless Components Letters, vol. 16, no. 5, pp. 275–277, May 2006, doi: 10.1109/lmwc.2006.873504.
- [14]. Sarma, K. Sarmah, and K. K. Sarma, "Low return loss slotted rectangular microstrip patch antenna at 2.4 GHz," 2015 2nd International Conference on Signal Processing and Integrated Networks (SPIN), pp. 35–39, Feb. 2015, doi: 10.1109/spin.2015.7095333.
- [15]. J. Geng and Y. Zhai, "Research and Application of Prediction Model Based on Random Forest Algorithm," 2023 IEEE 3rd International Conference on Data Science and Computer Application (ICDSCA), pp. 935–938, Oct. 2023, doi: 10.1109/icdsca59871.2023.10393439.

Publisher's note: The publisher remains neutral with regard to jurisdictional claims in published maps and institutional affiliations. The content is solely the responsibility of the authors and does not necessarily reflect the views of the publisher.